JOURNAL OF CATALYSIS **172,** 187–193 (1997)
ARTICLE NO. CA971843

# A New Method of Analysing Temperature-Programmed Desorption (TPD) Profiles Using an Extended Integral Equation

K. Koch, B. Hunger,[1] O. Klepel, and M. Heuchel

*Institute of Physical and Theoretical Chemistry, University of Leipzig, D-04103 Leipzig, Germany*

Received April 21, 1997; revised July 8, 1997; accepted July 10, 1997

**A new method of analysing temperature-programmed desorption (TPD) profiles is suggested. Taking into account desorption curves of different heating rates it is shown that the desorption energy distribution function can be calculated by using an extended integral equation without any limiting assumptions about the distribution function and the preexponential factor. The method is demonstrated with simulated data and tested for TPD of different molecules on zeolites.** © 1997 Academic Press

## INTRODUCTION

Temperature-programmed desorption (TPD) is a frequently used method to investigate the interaction of different adsorbate molecules with catalyst surfaces. However, in the case of porous catalysts a quantitative interpretation of desorption profiles is difficult because diffusion and readsorption effects may influence the observed rate of desorption. By means of model calculations it could be shown that in this case the observed overall desorption rate $r_d(T)$ for a desorption step of first order on a homogeneous surface can be described by the approximation (1–3)

$$r_d(T) = -\frac{d\theta}{dt} = k_{eff}\theta = \frac{\pi^2 D_{eff} k_d}{R_p^2 \nu_m k_a}\theta, \qquad [1]$$

where $\theta$ is the average degree of coverage and $k_{eff}$ is the effective desorption rate constant. $D_{eff}$ is the effective diffusion coefficient, $R_p$ is the mean particle radius of the catalyst pellets, $\nu_m$ is the initial concentration of the probe molecule adsorbed, and $k_d$ and $k_a$ are the rate constants for desorption and adsorption, respectively. The temperature dependence of the effective desorption rate constant can be expressed in terms of an Arrhenius equation:

$$k_{eff} = A\exp(-E/RT). \qquad [2]$$

It contains contributions from the effective diffusion coefficient (activation energy of diffusion) and the adsorption equilibrium constant (heat of adsorption). By means of NMR diffusion measurements on zeolitic adsorbate-adsorbent systems it was proved that the activation energy of long-range self-diffusion and the isosteric heat of adsorption coincide (4). From these results it may be concluded that the temperature dependence of the effective desorption rate constant is mainly determined by the heat of adsorption (in the following designated as desorption energy $E$). This agreement was found, e.g., for the desorption of different molecules on zeolites (e.g., (5–7)). In Eq. [2] $A$ is an effective preexponential factor.

Most of the real catalyst systems are energetically heterogeneous and therefore they show complex desorption profiles with multiple peaks and shoulders. This energetic heterogeneity is often taken into account by assuming a dependence of the desorption energy and the preexponential factor on the coverage (e.g., (8–10)). For that various algorithms of analysis were developed, resulting from different assumptions or requiring different experimental data (e.g., (11–14)). Another possibility to describe desorption from an energetically heterogeneous surface is to introduce a distribution function $f(E)$ of the desorption energy (e.g., (15–17)). Considering a desorption of first order with a desorption energy $E$ as the local desorption model the overall desorption rate $r_d(T)$ can be expressed by

$$r_d(T) = A\int_{E_{min}}^{E_{max}} \theta_{loc}(E,T)\exp(-E/RT)\,f(E)\,dE, \qquad [3]$$

where $\theta_{loc}$ is the local coverage on sites characterized by a desorption energy $E$; $E_{min}$ and $E_{max}$ are the limits of the range of desorption energy. The estimation of the distribution function can be carried out by several methods. Beside the curve fitting of model distributions (15), and model calculations by means of the Monte-Carlo method (18, 19), a direct numerical determination based on the regularization method is applicable (20, 21). This method does not require any limiting assumptions about the distribution function. In a recent paper (22), it was shown that, if the preexponential factor $A$ (assumed to be constant) is known, this numerical technique allows the calculation of the distribution

[1] Author for correspondence. E-mail: hunger@sonne.tachemie.uni-leipzig.de.



0021-9517/97 $25.00

function of the desorption energy resulting in an adequate description of the experimentally observed course of desorption. However, in most cases the preexponential factor is unknown. Therefore, it is the aim of this contribution to suggest a new method for the estimation of the desorption energy distribution function $f(E)$ which does not require the determination of the preexponential factor $A$ by means of other methods or model calculations.

## THEORY

The desorption integral equation [3] can be written in the form

$$r_d(T) = \int_{E_{min}}^{E_{max}} K(E, T)\, f(E)\, dE. \qquad [4]$$

From the mathematical point of view this is a linear Fredholm integral equation of the first kind with a general expression like (23)

$$g(y) = \int_a^b K(x, y)\, f(x)\, dx. \qquad [5]$$

The function $K(x, y)$ is called the kernel function of the integral equation. In our case this is the local desorption model, $g(y)$ is the experimentally determined overall desorption rate $r_d(T)$, and $f(x)$ is the desorption energy distribution function $f(E)$ which is the interesting quantity to characterize the catalyst surface.

Numerical solution of Eq. [5] requires its discretization by an appropriate quadrature method (24). This provides the system of linear equations

$$g(y_i)_{i=1\ldots m} = \int_a^b K(x, y_i)\, f(x)\, dx \simeq \sum_{j=1}^{n} w_j K_{ij} f_j, \qquad [6]$$

where $\boldsymbol{g}(y_i)_{i=1\ldots m}$ is the vector of experimental data, $m$ is the number of points, $n$ is the number of quadrature intervals, $\boldsymbol{x} = (x_j)_{1\ldots n}$ is the vector of interpolation nodes of the integration range $[a, b]$ and $\boldsymbol{w} = (w_j)_{1\ldots n}$ are the quadrature weights. $\boldsymbol{K}_{ij} = K(x_j, y_i)$ and $\boldsymbol{f}_j = f(x_j)$ are the discretized kernel and distribution function, respectively. Introducing

$$\boldsymbol{w} = \mathrm{diag}(w), \qquad \boldsymbol{K} = (K_{ij}), \qquad \boldsymbol{B} = K\boldsymbol{w}, \qquad [7]$$

one obtains the matrix formulation of the linear system

$$\boldsymbol{g} = \boldsymbol{B}\boldsymbol{f}. \qquad [8]$$

Usually such problems are solved by the Gaussian algorithm by means of minimization of the least squares,

$$//\boldsymbol{B}\boldsymbol{f} - \boldsymbol{g}//^2 \quad \text{minimize with respect to } \boldsymbol{f}, \qquad [9]$$

where $//\cdots//$ denotes the Euclidian vector norm. Within this approach one obtains the well-known solution

$$\boldsymbol{f} = (\boldsymbol{B}^T\boldsymbol{B})^{-1}\boldsymbol{B}^T\boldsymbol{g}. \qquad [10]$$

Unfortunately, this simple principle is, in general, not appropriate for the solution of Fredholm integral equations, because we are concerned with a so-called "ill-posed" problem (21). This means that errors in the measured values $g(y)$ and numerical uncertainties in the calculation lead to disturbances of the solution function $f(x)$ in such a way that it is impossible to extract any useful information.

One possibility to overcome this problem is to utilize the regularization method (21, 25). Within this method the minimizing condition is extendend as

$$//\boldsymbol{B}\boldsymbol{f} - \boldsymbol{g}//^2 + \gamma //\boldsymbol{C}\boldsymbol{f}//^2 \quad \text{minimize with respect to } \boldsymbol{f}. \qquad [11]$$

I.e., in addition to the minimum of the least squares there is another restriction for the solution. In the simplest case $\boldsymbol{C}$ is the unit matrix. Then the sum of the square of the target function is minimized, leading to a suppression of the disturbances. Another type of matrices used for $\boldsymbol{C}$ is the discretized differential matrix of second order. This leads to a minimization of the curvature of the function $\boldsymbol{f}$ and thus to a smooth solution. The regularization parameter $\gamma$ adjusts the weight of the smoothing and has to be chosen carefully with respect to the experimental data (21, 26). The derivation of the solution equation results in

$$\boldsymbol{f} = (\boldsymbol{B}^T\boldsymbol{B} + \gamma\boldsymbol{C}^T\boldsymbol{C})^{-1}\boldsymbol{B}^T\boldsymbol{g}. \qquad [12]$$

This equation can be solved usefully by means of the singular value decomposition (27).

The estimation of the desorption energy distribution function from experimental TPD data, i.e., solution of Eq. [3], requires the calculation of the integral kernel $K(E,T)$ defined in Eq. [4]. For that the preexponential factor $A$ must be known (20–22). In this paper we propose a new method which allows the calculation of the distribution function without any a priori knowledge about $A$. Our new method is based on the following consideration: Accepting that the residual $r = //\boldsymbol{B}\boldsymbol{f} - \boldsymbol{g}//^2$ characterizes the deviation of the calculated overall desorption rate, represented by $\boldsymbol{B}\boldsymbol{f}$, from the measured desorption rate ($\boldsymbol{g}$), $r$ should be a minimum for an "optimal" preexponential factor. By varying $A$ over a certain range and calculating the desorption energy distribution function and the residual $r$, the minimum of $r$ should occur at the optimum of $A$.

The smoothing of the data by regularization which is necessary because of the ill-posedness of the problem leads to difficulties in finding the minimum of $r$. These problems can be solved by an improved method for the solution of the desorption integral equation which is based on an extended data basis analogous to the determination of adsorption energy distributions using adsorption measurements at different temperatures (28). By using simultaneously several desorption curves with $k$ different heating rates $Q_l$ (linear temperature program: $T = T_0 + Q_l t$; $l = 1, 2, \ldots, k$) it is

possible to use the integral equation which is a direct extension of Eq. [3],

$$r_d(T)_{Q_k} = A \int_{E_{min}}^{E_{max}} \theta_{loc}(E, T)_{A_0} \exp(-E/RT)\, f(E)\, dE. \quad [13]$$

In this equation an array of $k$ desorption curves is used for $r_d(T)$. The kernel function $K(E,T)$ has to be calculated for the appropriate values of $Q_k$. For the calculation of the energy distribution function the following system of linear equations has to be solved:

$$\begin{bmatrix} r_d(T)_{Q_1} \\ r_d(T)_{Q_2} \\ \vdots \\ r_d(T)_{Q_k} \end{bmatrix} = \begin{bmatrix} \boldsymbol{B}(E_1)_{Q_1} & \boldsymbol{B}(E_2)_{Q_1} & \cdots & \boldsymbol{B}(E_n)_{Q_1} \\ \boldsymbol{B}(E_1)_{Q_2} & \boldsymbol{B}(E_2)_{Q_2} & \cdots & \boldsymbol{B}(E_n)_{Q_2} \\ & \vdots & & \\ \boldsymbol{B}(E_1)_{Q_k} & \boldsymbol{B}(E_2)_{Q_k} & \cdots & \boldsymbol{B}(E_n)_{Q_k} \end{bmatrix} \boldsymbol{f}. \quad [14]$$

The resulting desorption energy distribution function $f(E)$ has to describe all $k$-measured desorption curves.

## RESULTS AND DISCUSSION

At first we have tested the above proposed approach using simulated data. For that a constant preexponential factor of $A = 1 \times 10^6$ min$^{-1}$ and a desorption energy distribution consisting of two Gaussian peaks ($E_1 = 55$ kJ mol$^{-1}$, standard deviation = 5 kJ mol$^{-1}$, relative frequency = 80%, $E_2 = 70$ kJ mol$^{-1}$, standard deviation = 5 kJ mol$^{-1}$, relative frequency = 20%) were used. Considering a desorption of first-order, desorption curves for different heating rates ($1 \cdots 20$ K min$^{-1}$) were calculated by use of Eq. [3]. To the theoretically calculated desorption curves random errors of about 1% were added. For all calculations the regularization parameter $\gamma$ was taken to $5 \times 10^{-3}$.

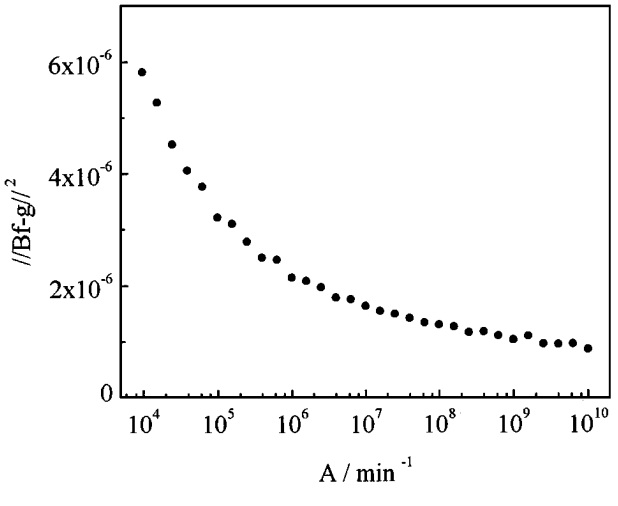


**FIG. 1.** Dependence of the residual $//\boldsymbol{Bf} - \boldsymbol{g}//^2$ on the preexponential factor $A$ using a single desorption curve (2 K min$^{-1}$).

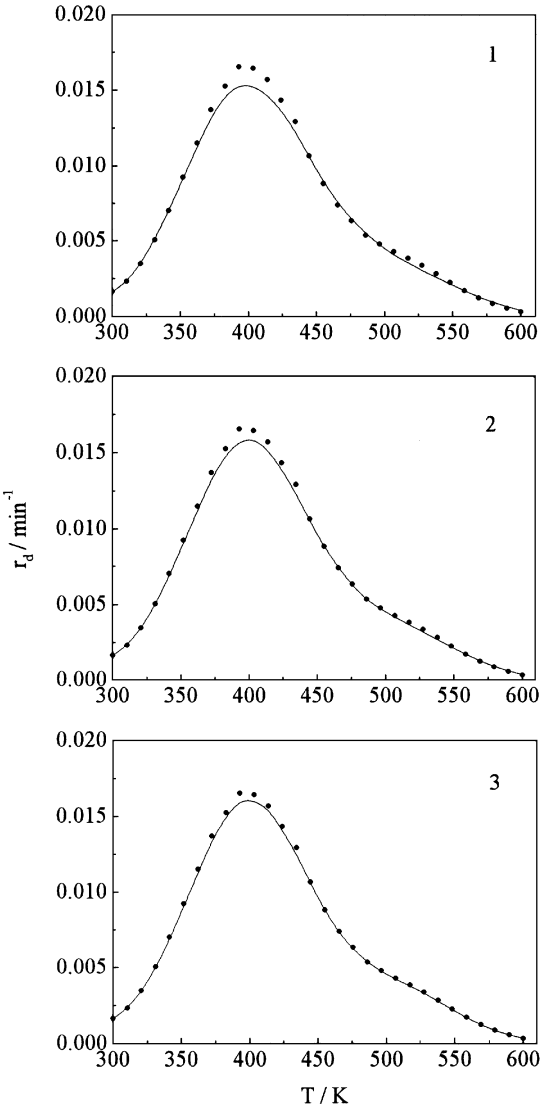


**FIG. 2.** Calculated desorption curves in dependence on the preexponential factor (2 K min$^{-1}$: ●, simulated data; ———, calculated data). 1. $A = 1 \times 10^4$ min$^{-1}$; 2. $A = 1 \times 10^6$ min$^{-1}$; 3. $A = 1 \times 10^{10}$ min$^{-1}$.

Using only a single desorption curve the calculation of $f(E)$ was carried out for the range of $A$ from $1 \times 10^4$ to $1 \times 10^{10}$ min$^{-1}$. Figure 1 shows that for a heating rate of 2 K min$^{-1}$ an increase of $A$ results in a decreasing residual, but there is no minimum. From these results it may be concluded that the complex form of the energy distribution allows a fairly accurate description of the measured data with increasing $A$ (Fig. 2), but no additional information can be obtained regarding the preexponential factor from a single desorption curve.

However, if desorption curves with different heating rate are analyzed simultaneously with the model of the desorption energy distribution functions (Eq. [13]), the result is different. As can be seen from Fig. 3, the dependence of the residual on the value of the preexponential factor $A$

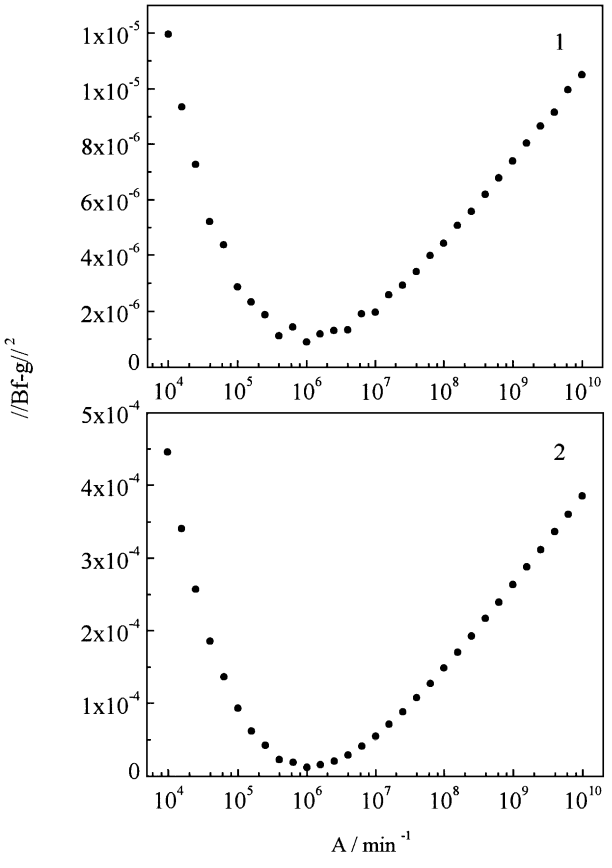


**FIG. 3.** Dependence of the residual $//\boldsymbol{Bf} - \boldsymbol{g}//^2$ on the preexponential factor using different desorption curves. 1. 2, 4 K min$^{-1}$; 2. 2, 4, 6, 8, 10, 12, 14 K min$^{-1}$.

shows a minimum. With the increasing number of desorption profiles the minimum becomes deeper. The location of the minimum at about $A = 1.0 \times 10^6$ min$^{-1}$, the assumed value for the simulated data, remains unchanged. Only with this $A$ and the calculated desorption energy distribution (see Fig. 4), which is in quantitative agreement with the initially assumed distribution function, it was possible to reproduce optimally the course of desorption for all used heating rates, as can be seen from Fig. 5.

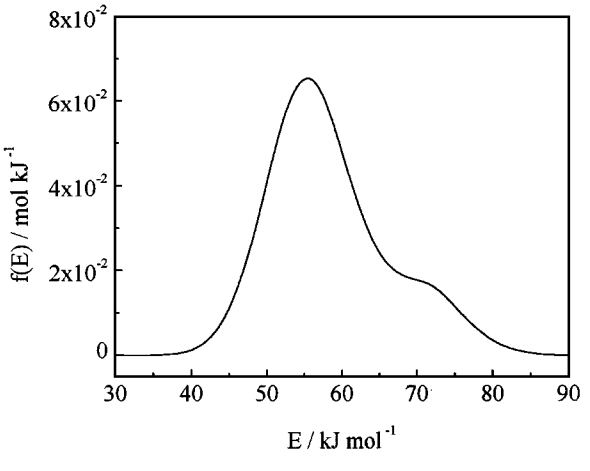


**FIG. 4.** Calculated desorption energy distribution for $A = 1 \times 10^6$ min$^{-1}$.

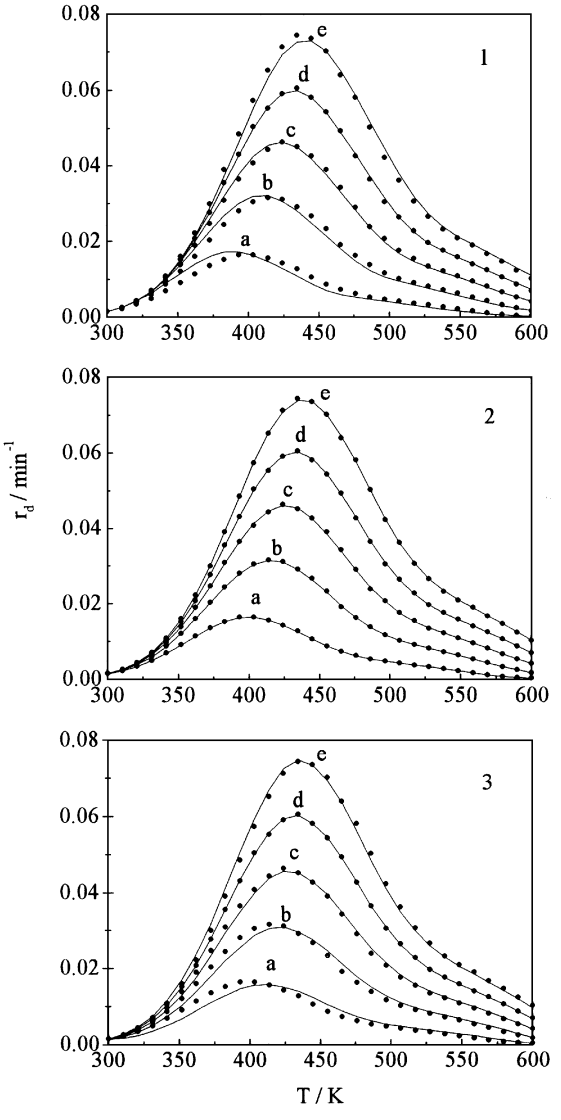


**FIG. 5.** Calculated desorption curves in dependence on the preexponential factor (●, simulated data; ———, calculated data). 1. $A = 1 \times 10^4$ min$^{-1}$; 2. $A = 1 \times 10^6$ min$^{-1}$; 3. $A = 1 \times 10^{10}$ min$^{-1}$; a. 2 K min$^{-1}$; b. 4 K min$^{-1}$; c. 6 K min$^{-1}$; d. 8 K min$^{-1}$; e. 10 K min$^{-1}$.

Further, the proposed analysis was tested for TPD of different molecules on zeolites: $H_2O$/Na$X$(Si/Al = 1.18), $NH_3$/HZSM-5(Si/Al = 28) and $N$-methyl-pyrrolidine/HNa$Y$(Si/Al = 2.6, exchange degree = 88%). The experiments were performed in a flow device with helium as carrier gas (3 liters h$^{-1}$). For evolved gas detection a thermal conductivity detector ($H_2O$, $N$-methyl-pyrrolidine) and a flame ionization detector ($NH_3$) were used. The zeolites were loaded at different temperatures ($H_2O$: 300 K, $N$-methyl-pyrrolidine: 323 K, $NH_3$: 523 K) and flushed with helium until no further desorption could be observed at this

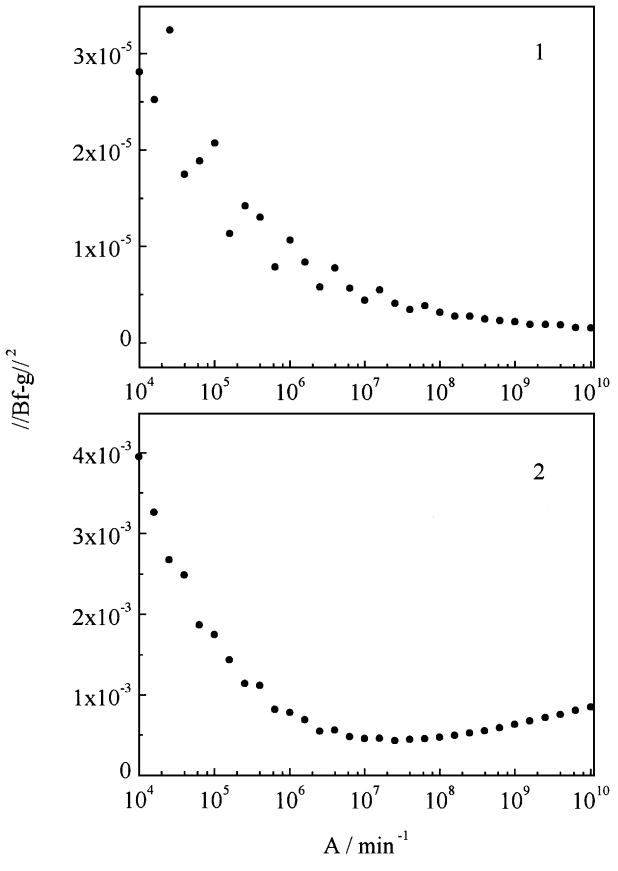


**FIG. 6.** Dependence of the residual $//\boldsymbol{Bf}-\boldsymbol{g}//^2$ on the preexponential factor using different desorption curves for water desorption on Na$X$. 1. 1.5 K min$^{-1}$; 2. 1.5, 3, 7.8, 13.2, 19.8 K min$^{-1}$.

temperature. TPD was carried out with a linear temperature program and different heating rates (1–20 K min$^{-1}$). Further details are given in (19, 29).

Beside the residual curve obtained by using a single TPD profile of water on Na$X$ (desorbed amount: $10 \pm 1$ mmol g$^{-1}$) in Fig. 6 an example with five different heating rates is shown. As for the simulated data, only in case of an analysis including curves with several heating rates a minimum of the residual appears at $A = 2.5 \times 10^7$ min$^{-1}$. The relatively flat shape of this minimum is probably caused by the limited accuracy of the experimentally determined desorption profiles. Figure 7 shows the calculated desorption curves in comparison with the experimental data for three selected values of the preexponential factors. It can be seen clearly that only for an $A$ value corresponding to the residual minimum an optimal representation of all desorption curves with the calculated desorption energy distribution function of Fig. 8 is possible. For other $A$ values larger deviations from the experimental curves appear, especially at lower heating rates. Taking into account the error of these investigations, the obtained value of $A$ ($2.5 \times 10^7$ min$^{-1}$) corresponds to the range of $A$ ($7 \times 10^6$–$2 \times 10^7$ min$^{-1}$) which was approximately estimated by means of the dependence of the peak temperature (main peak) on the heating rate (29). The energy range of about 45 kJ mol$^{-1}$ to 90 kJ mol$^{-1}$ of the calculated desorption energy distribution in Fig. 8

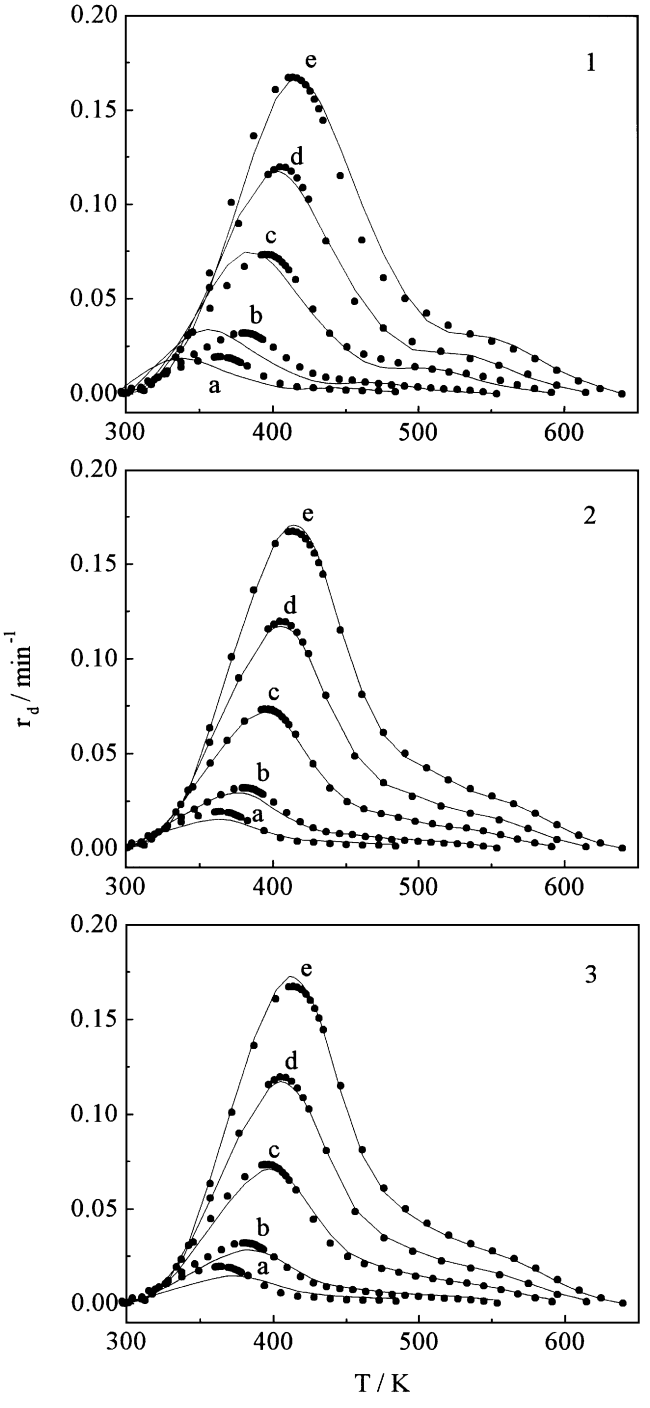


**FIG. 7.** Calculated desorption curves of water desorption on Na$X$ in dependence on the preexponential factor (●, experimental data; ———, calculated data). 1. $A = 1 \times 10^4$ min$^{-1}$, 2. $A = 2.5 \times 10^7$ min$^{-1}$; 3. $A = 1 \times 10^{10}$ min$^{-1}$; a. 1.5 K min$^{-1}$; b. 3 K min$^{-1}$; c. 7.8 K min$^{-1}$; d. 13.2 K min$^{-1}$; e. 19.8 K min$^{-1}$.

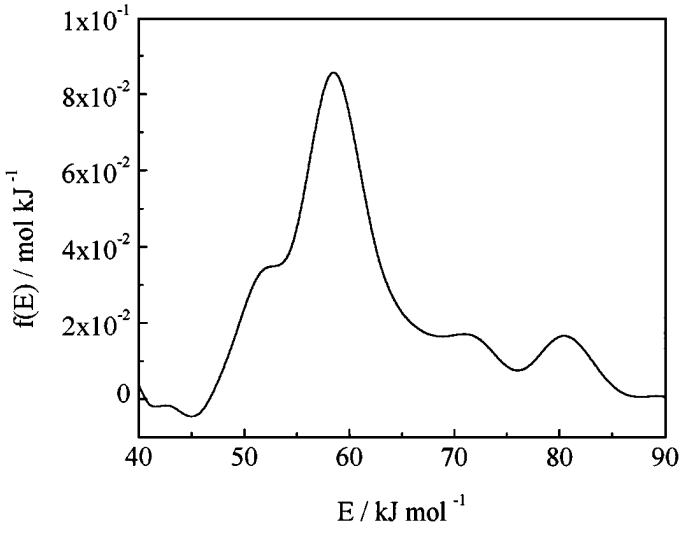


**FIG. 8.** Calculated desorption energy distribution of water desorption on Na$X$ ($A = 2.5 \times 10^7$ min$^{-1}$).

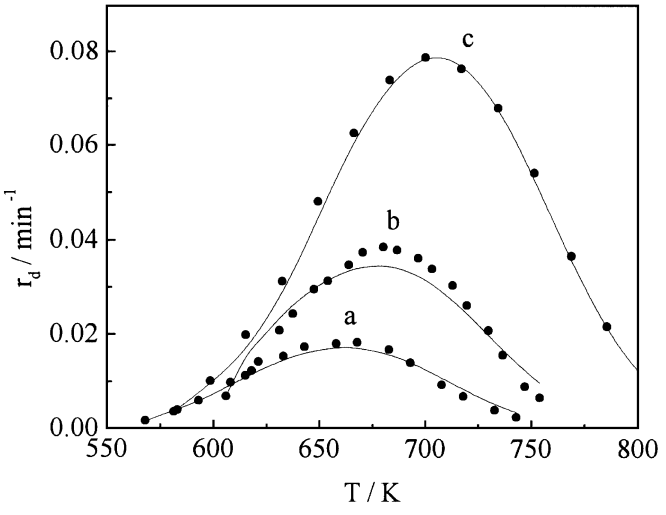


**FIG. 10.** Calculated desorption curves of ammonia desorption on HZSM-5 ($A = 3 \times 10^9$ min$^{-1}$: ●, experimental data; ———, calculated data); a. 2 K min$^{-1}$; b. 4 K min$^{-1}$; c. 10 K min$^{-1}$.

is in good agreement with heats of adsorption determined with microcalorimetry (e.g., (30)), and it shows clearly the energetic heterogeneity of interaction of water with this zeolite.

The new method was tested with two further examples. Figures 9–11 show the results for TPD of ammonia on a HZSM-5 zeolite (desorbed amount: 0.28 mmol g$^{-1}$) and Fig. 12 presents the calculated desorption energy distribution for TPD of *N*-methyl-pyrrolidine on a HNaY zeolite (desorbed amount: 1.2 mmol g$^{-1}$) by use of three heating rates (2, 4, and 10 K min$^{-1}$). For both examples (see Figs. 9 and 12), the dependence of the residual on the value of the preexponential factor shows a minimum. This result indicates that in each case the course of desorption of all used heating rates can be described optimally with a constant value of $A$.

The estimated preexponential factor ($A = 3 \times 10^9$ min$^{-1}$) and the shape and the position of the desorption energy distribution of ammonia desorption on HZSM-5, which can be attributed to the interaction of ammonia with the bridging SiOHAl groups of the zeolite, are in good agreement with our previous results ($A = 4.9 \times 10^9$–$2 \times 10^{10}$ min$^{-1}$) (19, 22). The energy range of the distribution function (120–160 kJ mol$^{-1}$) is in accordance with results of calorimetric studies at comparable loadings (e.g., (31, 32)).

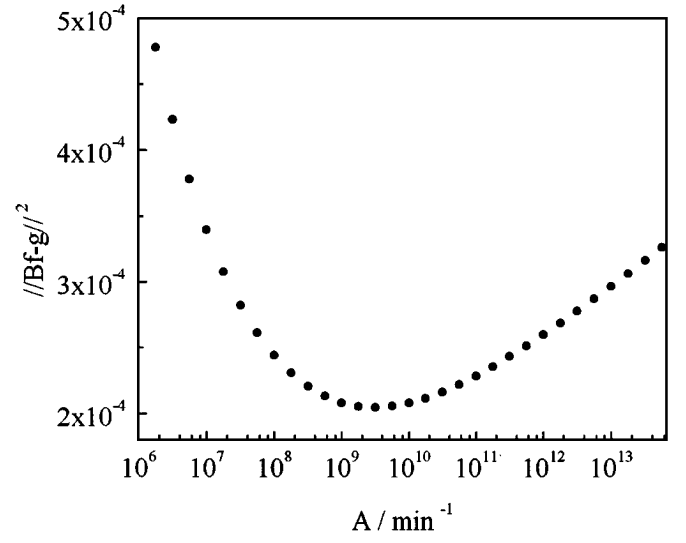


**FIG. 9.** Dependence of the residual $//\boldsymbol{Bf} - \boldsymbol{g}//^2$ on the preexponential factor using different desorption curves for ammonia desorption on HZSM-5 (2, 4, and 10 K min$^{-1}$).

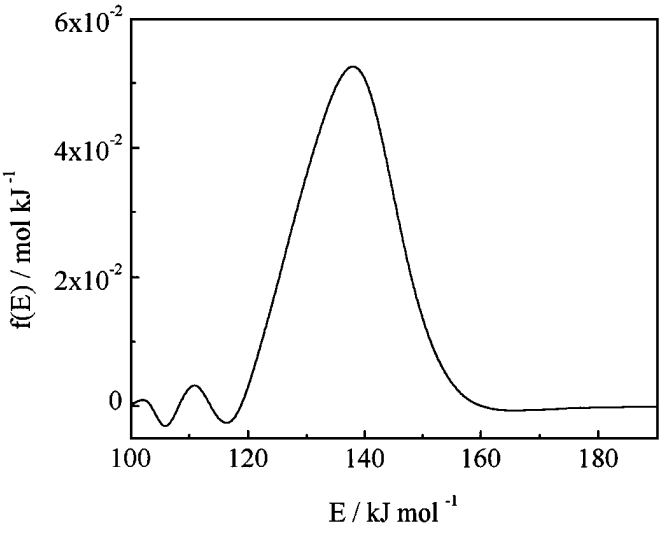


**FIG. 11.** Calculated desorption energy distribution of ammonia desorption on HZSM-5 ($A = 3 \times 10^9$ min$^{-1}$).

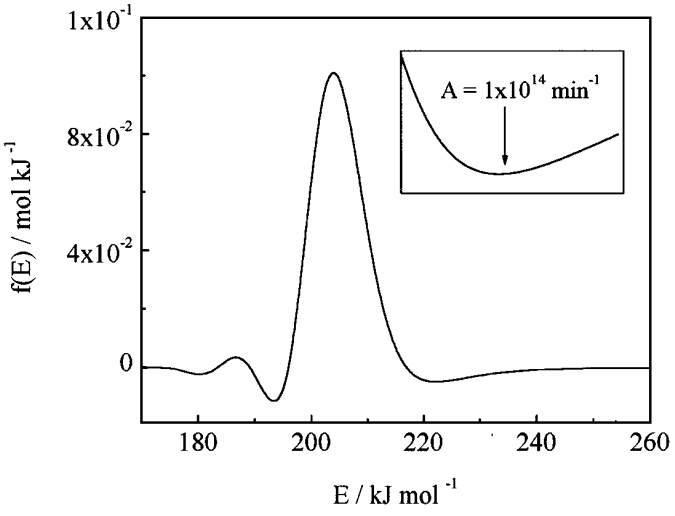


**FIG. 12.** Calculated desorption energy distribution of *N*-methyl-pyrrolidine desorption on HNa*Y*.

In case of TPD of *N*-methyl-pyrrolidine on HNa*Y* the obtained value of the preexponential factor ($A = 1 \times 10^{14}$ min$^{-1}$) corresponds to the results of our previous studies ($A = 1 \times 10^{15}$ min$^{-1}$) (33). The deviations are in the range of the errors. It follows that the position of the maximum of the distribution function shifts about 10 kJ mol$^{-1}$. However, up to now, no adsorption heats are for comparison of these results available.

The proposed method should be a useful tool to obtain information about the interaction strength of adsorbate molecules from TPD experiments, easily and quickly, and without further assumptions. Using about 3–5 different heating rates, the accuracy of the experiments allows the estimation of the preexponential factor in the range of about one order of magnitude. An improvement of this analysis could consist in considering a distribution or coverage dependence, respectively, of the preexponential factor $A$, because an assumption of a constant value should not be adequate in many cases (e.g., (10)). Using the relationship between the preexponential factor and the desorption energy according to the compensation effect ($\ln A(\theta) = bE(\theta) + c$, where $b$ and $c$ are constants) (9, 34), we have carried out some test calculations. These investigations have shown that the resulting $A$ is an effective value located in the assumed range of the preexponential factor. However, an estimation of the dependence of the preexponential factor on the coverage or on the desorption energy, respectively, needs further experimental information about the desorption process, e.g., experiments using different initial coverages for each set of heating rates. In this context further investigations are necessary.

## ACKNOWLEDGMENT

The authors gratefully acknowledge the financial support of the Fonds der Chemischen Industrie and the Deutsche Forschungsgemeinschaft, Graduate College "Physical Chemistry of Interfaces."

## REFERENCES

1. Demmin, R. A., and Gorte, R. J., *J. Catal.* **90**, 32 (1984).
2. Tronconi, E., and Forzatti, P., *J. Catal.* **93**, 197 (1985).
3. Tronconi, E., and Forzatti, P., *Chem. Engng. Sci.* **42**, 2779 (1987).
4. Kärger, J., and Ruthven, D. M., "Diffusion in Zeolites," Wiley, New York, 1992.
5. Richards, R. E., and Rees, L. V. C., *Zeolites* **6**, 17 (1986).
6. Hunger, B., and von Szombathely, M., *Z. Phys. Chem.* **190**, 19 (1995).
7. Hunger, B., Heuchel, M., Matysik, S., and Einicke, W.-D., *Thermochim. Acta* **269/270**, 599 (1995).
8. King, D. A., *Surf. Sci.* **47**, 384 (1975).
9. de Jong, A. M., and Niemantsverdriet, J. W., *Surf. Sci.* **233**, 355 (1990).
10. Zhdanov, V. P., *Surf. Sci. Rep.* **12**, 183 (1991).
11. Falconer, J. L., and Madix, R. J., *Surf. Sci.* **48**, 393 (1975).
12. Forzatti, P., Borghesi, M., Pasquon, I., and Tronconi, E., *Surf. Sci.* **137**, 595 (1984).
13. Hunger, B., and Hoffmann, J., *Thermochim. Acta* **106**, 133 (1986).
14. Dima, E., and Rees, L. V. C., *Zeolites* **7**, 219 (1987).
15. Carter, G., *Vacuum* **12**, 245 (1962).
16. Dondur, V., and Fidler, D., *Surf. Sci.* **150**, 480 (1985).
17. Karge, H. G., and Dondur, V., *J. Phys. Chem.* **94**, 765 (1990).
18. Sales, J. L., and Zgrablich, G., *Surf. Sci.* **187**, 1 (1987).
19. Hunger, B., Hoffmann, J., Heitzsch, O., and Hunger, M., *J. Thermal Anal.* **36**, 1379 (1990).
20. Bischke, S. D., Chemburkar, R. M., Brown, L. F., and Travis, B. J., *in* "Fundamentals of Adsorption—Proceedings of the Third International Conference on Fundamentals of Adsorption" (A. B. Mersmann and S. E. Scholl, Eds.), p. 145. Engineering Foundation, New York Deutsche Vereinigung für Chemie- und Verfahrenstechnik, Frankfurt/Main, 1991.
21. von Szombathely, M., Bräuer, P., and Jaroniec, *J. Comput. Chem.* **13**, 17 (1992).
22. Hunger, B., von Szombathely, M., Hoffmann, J., and Bräuer, P., *J. Thermal Anal.* **44**, 293 (1995).
23. Bronstein, I. N., and Semendiajew, K. A., "Taschenbuch der Mathematik" Teubner, Leipzig, 1985.
24. Schwarz, H. R., "Numerische Mathematik," Teubner, Stuttgart, 1993.
25. Tikhonov, A. N., *Dokl. Akad. Nauk USSR* **39**, 195 (1943).
26. Hansen, P. Ch., *Inverse Problems* **8**, 849 (1992).
27. Golub, G. H., and Reinsch, C., *Numer. Math.* **14**, 403 (1970).
28. von Szombathely, M., Koch, K., and Neugebauer, N., *in* "Fundamentals of Adsorption—Proceedings of the Fifth International Conference on Fundamentals of Adsorption" (M. D. Le Van, Ed.), p. 921. Kluwer Academic, Boston, 1996.
29. Hunger, B., Matysik, S., Heuchel, M., Geidel, E., and Toufar, H., *J. Thermal Anal.* **49**, 553 (1997).
30. Dzhigit, O. M., Kiselev, A. V., Mikos, K. N., Muttik, G. G., and Rahmanova, T. A., *Trans. Faraday Soc.* **67**, 458 (1971).
31. Sayed, M. B., Auroux, A., and Vedrine, J. C., *Appl. Catal.* **23**, 49 (1986).
32. Kapustin, G. I., Brueva, T. R., Klyachko, A. L., Beran, S., and Wichterlová, B., *Appl. Catal.* **42**, 239 (1988).
33. Hunger, B., and von Szombathely, M., *Stud. Surf. Sci. Catal. A* **84**, 669 (1994).
34. Niemantsverdriet, J. W., Markert, K., and Wandelt, K., *Appl. Surf. Sci.* **31**, 211 (1988).